

# SIMULATION-BASED FRAMEWORK TO DEVELOP A CONTROL SYSTEM FOR FUNCTIONAL ELECTRICAL STIMULATION

Minsik Hong

Dept. of Electrical and Computer Engineering  
University of Arizona  
1230 E Speedway Boulevard, Tucson, AZ, USA  
mshong@email.arizona.edu

Brady A. Hasse

Department of Neuroscience  
University of Arizona  
1040 4th St, Tucson, AZ, USA  
hasse2ba@email.arizona.edu

Andrew J. Fuglevand

Department of Physiology  
Department of Neuroscience  
University of Arizona  
1501 N Campbell, Tucson, AZ, USA  
fuglevan@email.arizona.edu

Jerzy W. Rozenblit

Dept. of Electrical and Computer Engineering  
Department of Surgery  
University of Arizona  
1230 E Speedway Boulevard, Tucson, AZ, USA  
jerzyr@arizona.edu

## ABSTRACT

Functional electrical stimulation (FES) has long been used to restore movements in paralyzed individuals. However, other than a small set of simple, preprogrammed movements, it has been challenging to accurately evoke natural movements with FES. This is due to the complexity of the system and moment-by-moment changes in the efficacy of stimulation and muscle fatigue. In this paper, a simulation-based design framework is proposed to develop and validate a FES control system that produces a wide range of complex upper limb movements. By using index finger motions with electromyographic signals as an example, we show the feasibility and effectiveness of the proposed framework to develop an advanced FES control system. Also, we show that error compensations could be used to command adjustments across a population of muscles to enhance movement accuracy.

**Keywords:** functional electrical stimulation, electromyography, rehabilitation, system identification, artificial neural networks.

## 1 INTRODUCTION

Functional electrical stimulation (FES) is a rehabilitative technology that serves to restore some degree of motor function in paralyzed individuals following spinal cord injury or stroke (Peckham and Knutson 2005). FES devices take advantage of the retained electrical excitability of the motor axons that innervate most paretic muscles. This residual function allows for the induction of muscle contraction through artificial stimulation delivered by surface electrodes, intramuscular electrodes, or by electrodes that encircle peripheral nerves supplying muscles. By stimulating combinations of muscles with a specific temporal pattern, useful motor responses can be elicited.

In existing FES systems (Memberg et al. 2014; Kilgore et al. 2008), only a few, simple, pre-programmed movements can be produced. This is largely due to the difficulty associated with identifying the intricate patterns of muscle activity needed to produce even relatively simple movements. Indeed, most natural movements require coordination of many muscles across multiple joints. To address this limitation, we developed a machine-learning method to predict the patterns of muscle activity that served as stimulation templates needed to produce a wide array of movements in paralyzed upper limbs (Hasse et al. 2022).

Many factors such as muscle fatigue and unaccounted for changes in the efficacy of stimulation with changes in limb configuration, however, affect the accuracy of the evoked movements. These errors can be significant and limit the practical utility of such artificial muscle stimulation. It seems crucial, therefore, to include some form of feedback (Crago, Nakai, and Chizeck 1991; Lynch and Popovic 2008; Blana, Kirsch, and Chadwick 2009; Wenger et al. 2014) to the open loop FES system we have developed to minimize evoked movement errors. A significant challenge for feedback control in the present context, however, is enacting real-time adjustments over large numbers of muscles based on sensed discrepancies between actual and desired trajectories.

Therefore, our goal is to develop a theoretical, simulation-based framework whereby detected errors in evoked arm movements could be used to command adjustments across a population of muscles needed to greatly enhance movement accuracy. Ultimately, success of this approach would be a major advance toward the realization of an upper-limb neuroprosthetic, enabling individuals with high level paralysis to use their own arms to interact with the environment in complex ways.

## 2 PROBLEM DEFINITION

In general, designing a FES control system is challenging due to system characteristics such as non-linearity, time varying, and complexity (e.g., a highly coupled system). Also, appropriate validation methods should be used to evaluate system performance and stability before deploying the system for actual human users as well as conducting experiments with human subjects.

In (Hasse et al. 2022), we proposed four sequential stages to develop a FES system. In stage 1, an artificial neural network (ANN) was trained given recorded limb kinematics and the corresponding electromyographic (EMG) signals. In stage 2, EMG signals were predicted using the trained ANN (i.e., EMG generator) given desired kinematics. In stage 3, stimulus pulses were generated by a FES converter which converts predicted EMG into stimulation. Finally, in stage 4, predicted stimulation patterns were delivered to 29 muscles controlling the upper limb in temporarily paralyzed monkeys to evaluate the FES system.

In this paper, we mainly focused on the relationship between EMG signals and desired movements rather than FES conversion. We assume that a FES converter will generate more accurate stimulus pulses if an EMG generator predicts elaborate muscle activities given a desired trajectory by minimizing movement errors. Also, we developed a nonlinear system identification model to provide a simulation setup which allows us to rigorously test the approach that otherwise would be difficult to do experimentally in monkeys or humans.

To demonstrate our approach, we used free movements of the human index finger controlled by six muscles. Figure 1 shows our proposed simulation system. The system consists of a nonlinear system model to

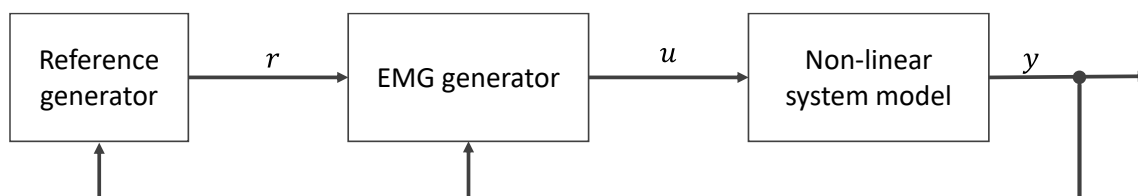


Figure 1. A simulated system for index finger control using EMG signals.

characterize index finger motions, an EMG generator to generate EMG signals ( $u$ ) given reference ( $r$ ) and system outputs ( $y$ ), and a reference generator to provide a desired trajectory.

### 3 SYSTEM MODELING

#### 3.1 Kinematic and EMG Data Collection and Processing

An electromagnetic tracking system (Liberty System, Polhemus Inc.) was used to record three degrees-of-freedom motion from the index finger of a human subject (xyz positions of the distal segment of the index finger; 120 Hz sampling rate). While recording finger movements, EMG signals were captured from all 6 muscles that insert into the index finger (first dorsal interosseus, FDI; first palmar interosseus, FPI; extensor indicis, EI; and index finger compartments of extensor digitorum, ED2; flexor digitorum superficialis, FDS2; and flexor digitorum profundus, FDP2). Bipolar intramuscular electrodes were used for all muscles except for first dorsal interosseus (accessible for surface electrode recording). EMG signals were sampled at 2500 Hz (CED Power 1401, Cambridge, UK). To align kinematics with EMG signals, we used synchronization pulses generated by the Polhemus system. We recorded about 20 minutes of EMG and kinematic data while the subject continuously moved the index finger along a self-determined random trajectory. Figure 2 depicts our experimental setup.

Collected data were postprocessed using MATLAB (MathWorks, Inc.). The recorded fingertip positions were normalized to finger length and low-pass filtered (4 Hz). EMG signals were full-wave rectified, low-pass filtered (4Hz) and normalized to the maximum amplitude recorded in the experimental session. Finally, EMG signals were down-sampled to synchronize with fingertip kinematics. These data were used to develop a nonlinear system model and an EMG generator as well as to conduct a simulation.

#### 3.2 Nonlinear System Identification

We derived a nonlinear system model to characterize a relationship between EMG signals and fingertip movements. This is a multiple-input and multiple-output (MIMO) nonlinear system. This system can be expressed by the NARMAX model (Chen, Billings, and Grant 1990):

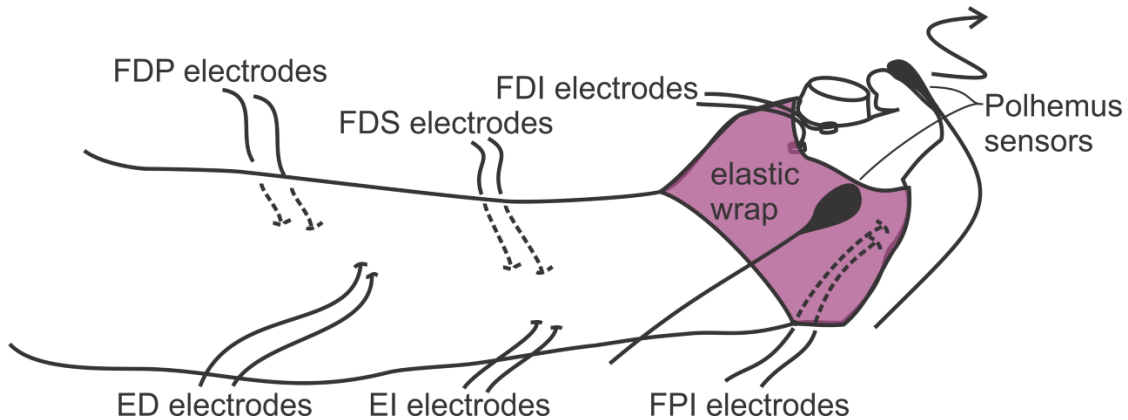


Figure 2. Experimental setup. Pairs of electrodes were led to differential amplifiers to record EMG signals from the six muscles controlling the index finger: FDP (flexor digitorum profundus), FDS (flexor digitorum superficialis), FDI (first dorsal interosseus), ED (extensor digitorum), EI (extensor indicis), FPI (first palmar interosseus). All electrodes were intramuscular except for FDI (which were surface electrodes). The hand and digits (except the index finger) were secured to a rigid cylinder with elastic wrap. Movements of the tip of the index finger were recorded with a 6 DOF Polhemus sensor (fixed to the fingernail with super glue) and registered relative to a Polhemus sensor placed at the base of the index finger.

$$y(k + 1) = f(y(k), y(k - 1), \dots, y(k - n + 1), u(k), u(k - 1), \dots, u(k - m + 1)) + d(k)$$

where  $y$ ,  $u$ ,  $d$  are the system output, input, and disturbance (e.g., uncorrelated noise), respectively.  $k$  represents a discrete time domain.  $n$  and  $m$  are the maximum lags of output and input, respectively.

Using the NARMAX model, our simplified system model can be expressed as follows:

$$\hat{y}(k + 1) = f(y(k), y(k - 1), y(k - 2), u(k))$$

where  $\hat{y}$  is an estimated fingertip position ( $\mathbb{R}^3$ ) given three lagged fingertip positions ( $y(k), y(k - 1), y(k - 2)$ ) with system input (EMG signals:  $u(k) \in \mathbb{R}^6$ ). We assume that the next output (predicted position,  $\hat{y}(k + 1)$ ) depends on the current control input ( $u(k)$ ) given three lagged positions where three lags allow us to capture position, velocity, and acceleration.

To model a function  $f$ , we used an artificial neural network (ANN). As a function approximator, ANNs can have one or more hidden layers given input and output layers. The feedforward network can predict  $\hat{y}$  using  $x(k) = (y(k), y(k - 1), y(k - 2), u(k))$ . Therefore, the ANN has 15 input nodes (where 9 for three lagged fingertip positions and 6 for EMG signals) and 3 output nodes (predicted position,  $\hat{y}$ ). Figure 3-(a) depicts the ANN architecture. We constructed a fully connected network using one hidden layer which has 64 nodes with Rectified Linear Unit (ReLU) activation functions. The number of hidden layers and its nodes were determined empirically.

### 3.3 EMG Generator

We also designed an ANN to predict EMG signals ( $\hat{u}$ ) given three lagged fingertip positions and a desired position ( $r$ ). The predicted  $\hat{u}$  can be described as follows:

$$\hat{u}(k) = g(r(k), y(k), y(k - 1), y(k - 2))$$

where  $r(k)$  is a desired next position at time  $k$  (i.e.,  $r(k) = y(k + 1)$ ) and  $g$  is a nonlinear function to characterize the relationship between muscle activities and kinematics. The ANN consists of 12 input nodes (3 for a desired position and 9 for three lagged fingertip positions), 4 hidden layers with 64 nodes and ReLU activation functions, and 6 output nodes (EMG for 6 muscles) as shown in Figure 3-(b).

### 3.4 Training Procedure

Both ANNs were trained using 40,000 samples with 10,000 epochs. The samples were randomly selected from the first half ( $\sim 70,000$ ) of the collected data ( $\sim 144,000$ ) as presented in section 3.1. For instance, each sample consists of  $y(k + 1), y(k), y(k - 1), y(k - 2)$ , and  $u(k)$ . To train the EMG generator, we used  $y(k + 1), y(k), y(k - 1), y(k - 2)$  as input of the network and  $u(k)$  as expected output of the network.

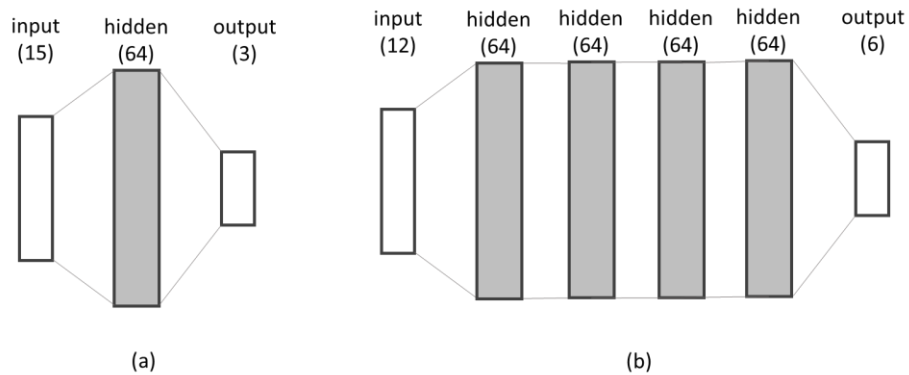


Figure 3. Fully connected ANN architectures for (a) the nonlinear system model to predict fingertip position and (b) the EMG generator.

An Adam optimizer (Kingma and Ba 2014) with a L1 loss function was used for this training (where  $\alpha$  (*learning rate*) = 0.0007 for the nonlinear model and  $\alpha = 0.0002$  for the EMG generator). ANNs were implemented using PyTorch (Paszke et al. 2019).

## 4 RESULTS

### 4.1 Methodology

ANNs were tested by using a test set which consists of 6,000 sequenced samples. The test samples were selected from the other half of the collected data. To evaluate the overall performance of both trained ANNs, the metrics used are coefficient of variation ( $R^2$ ), the root mean squared error (RMSE), and the mean absolute error (MAE). Also, we used qualitative measures by comparing between estimated outcomes and desired outcomes.

### 4.2 Nonlinear Model Validation

The ability of the trained ANN for the nonlinear system model to predict fingertip positions was evaluated using the test set. Figure 4-(a) shows overall predicted (blue) positions ( $\hat{y} = (\hat{x}, \hat{y}, \hat{z})$ ) for each axis with desired (red) positions ( $y = (x, y, z)$ ). The proposed model has small prediction errors ( $\hat{y} - y$ ) as shown in Figure 4-(b). For each axis,  $R^2 \approx 1$ ,  $RMSE \approx 0.0015$ , and  $MAE \approx 0.001$ . Figure 4-(c) depicts predicted positions for the last 500 sequenced samples (about 4s of data) and its 3D trajectory (blue) given a desired

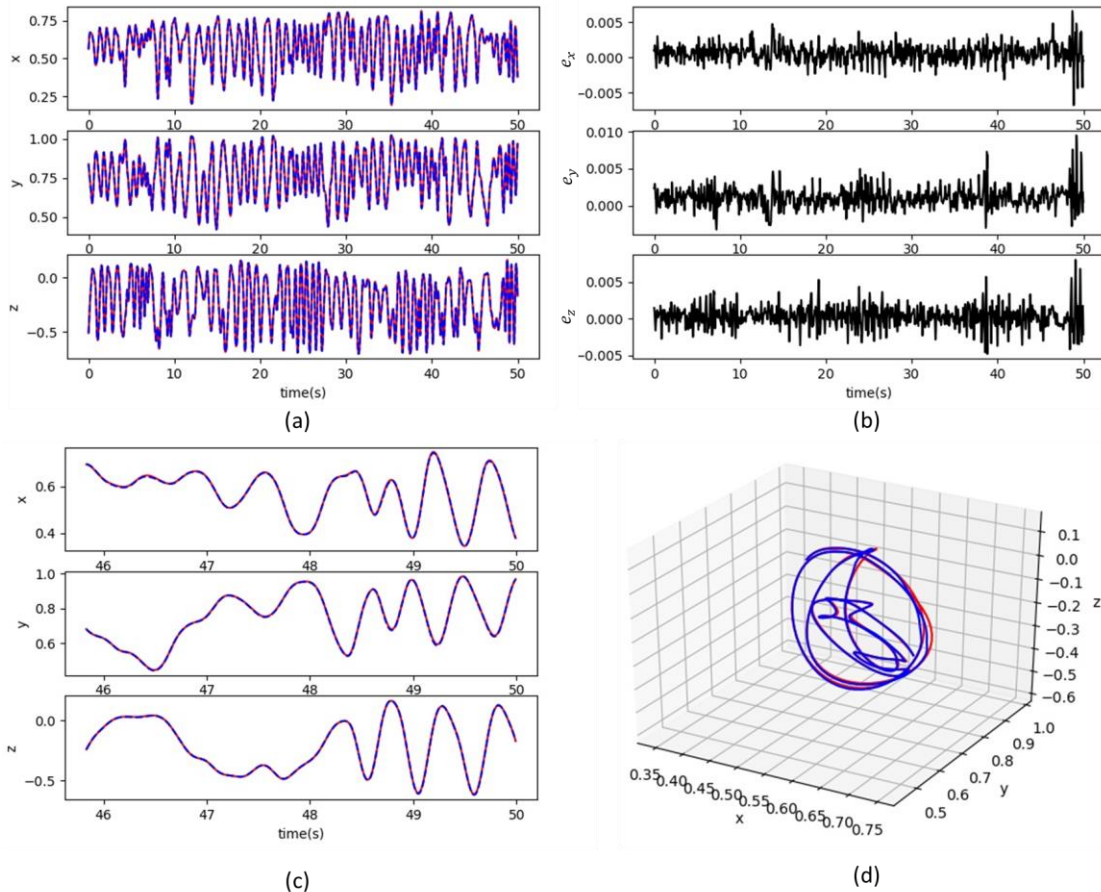


Figure 4. (a) actual (red) and predicted (blue) fingertip positions for 50s of test data. Red traces are almost completely overridden by highly accurate predicted (blue) position data, (b) error between  $y$  and  $\hat{y}$ , (c) actual and predicted positions over last 4s of data, and (d) 3D trajectories for the last 4s of data (where red:  $y$ , blue:  $\hat{y}$  in (a),(c),(d)).

Table 1. Evaluation metrics for the EMG generator

| Activation | Overall     |      |      | Partial (last 1,000 samples) |      |      |
|------------|-------------|------|------|------------------------------|------|------|
|            | $R^2$       | RMSE | MAE  | $R^2$                        | RMSE | MAE  |
| FDI        | <b>0.8</b>  | 0.07 | 0.05 | <b>0.83</b>                  | 0.06 | 0.04 |
| FPI        | 0.69        | 0.03 | 0.02 | 0.63                         | 0.04 | 0.03 |
| ED2        | 0.55        | 0.11 | 0.08 | 0.27                         | 0.15 | 0.11 |
| EI         | <b>0.75</b> | 0.09 | 0.07 | 0.53                         | 0.12 | 0.09 |
| FDP2       | 0.06        | 0.02 | 0.01 | 0.18                         | 0.03 | 0.02 |
| FDS2       | 0.04        | 0.03 | 0.02 | 0.03                         | 0.05 | 0.02 |

(red) trajectory is shown in Figure 4-(d). Compared to the overall predicted positions (i.e., 6,000 samples), the partial predicted one (i.e., the last 500 samples) has  $RMSE \approx 0.0023$ , and  $MAE \approx 0.0015$  for each axis. We found that lagged fingertip positions ( $y(k), y(k-1), y(k-2)$ ) were dominant when predicting positions (i.e., EMG signals ( $u(k)$ ) had no significant impact so that  $\hat{y}$  were estimated mostly based on three lagged outputs). For instance, when we used  $\hat{y}(k+1) = f(y(k), y(k-1), y(k-2), u(k) = 0)$  for all  $k$  (i.e., all EMG signals were zero),  $R^2 \approx 0.99$ ,  $RMSE \approx 0.004$ , and  $MAE \approx 0.0025$ .

### 4.3 EMG Generator Validation

The prediction ability of the EMG generator was also evaluated using the same test set. Figure 5-(a) shows the overall performance for six muscles where red is the actual and blue is the predicted EMG signals (after rectification, smoothing, and normalization). Predictions for FDI and EI activations were quite accurate ( $R^2 > 0.7$ ). However, FDP2 and FDS2 were inaccurate ( $R^2 \approx 0$ ). Figure 5-(b) shows predicted EMG for the last 8 s of data. The error metrics are summarized in Table 1. The poor predictions of FDP2 and FDS2 were likely due to migration of the deep intramuscular electrodes out of the muscle targets during the experiment. Such poor EMG predictions (i.e., the relationship between system states and EMG signals) likely affected the performance of the nonlinear system model.

### 4.4 Simulation Study

We next used the nonlinear model and the EMG generator with a reference generator to simulate a means to provide error compensation for an FES system. Among 6,000 test samples (i.e., movements for 50 seconds), we took a 1 second movement as a reference trajectory ( $y$ ). The simulation steps are as follows:

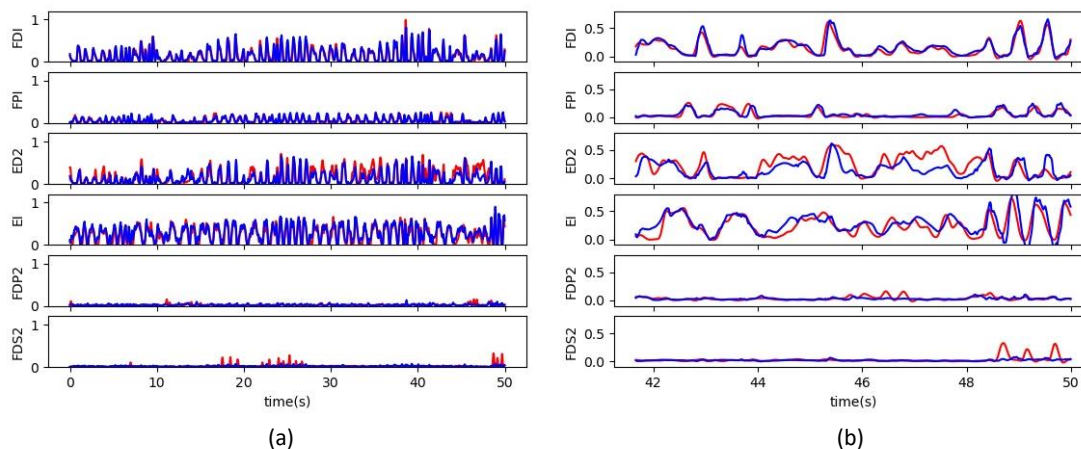


Figure 5. actual (red) and predicted (blue) EMG signals given (a) 6,000 test samples and (b) last 1,000 samples, respectively.

- Initialize  $\hat{y}(0), \hat{y}(-1), \hat{y}(-2)$
  - Repeat
    - Update  $r(k)$  with or without error compensation // reference generator
      - Without error compensation
 
$$r(k) = y(k + 1)$$
      - With error compensation
 
$$r(k) = \begin{cases} y(k + 1), & d < \delta \\ y(k + 1) + \alpha \cdot d \cdot \vec{v}, & d \geq \delta \end{cases}$$
- where  $d$  is a deviation between  $\hat{y}(k)$  and the reference trajectory and  $\vec{v}$  is a unit vector from  $\hat{y}(k)$  to  $y(k)$
- Update  $\hat{u}(k) = g(r(k), \hat{y}(k), \hat{y}(k - 1), \hat{y}(k - 2))$  // EMG generator
  - Update  $\hat{y}(k + 1) = f(\hat{y}(k), \hat{y}(k - 1), \hat{y}(k - 2), \hat{u}(k))$  // nonlinear model
  - Update  $\hat{y}(k), \hat{y}(k - 1), \hat{y}(k - 2)$

The purpose of this simulation was to verify that the EMG generator predicts EMG signals properly given a desired path so that we evaluate system performance and stability. Figure 6 shows the simulation results.

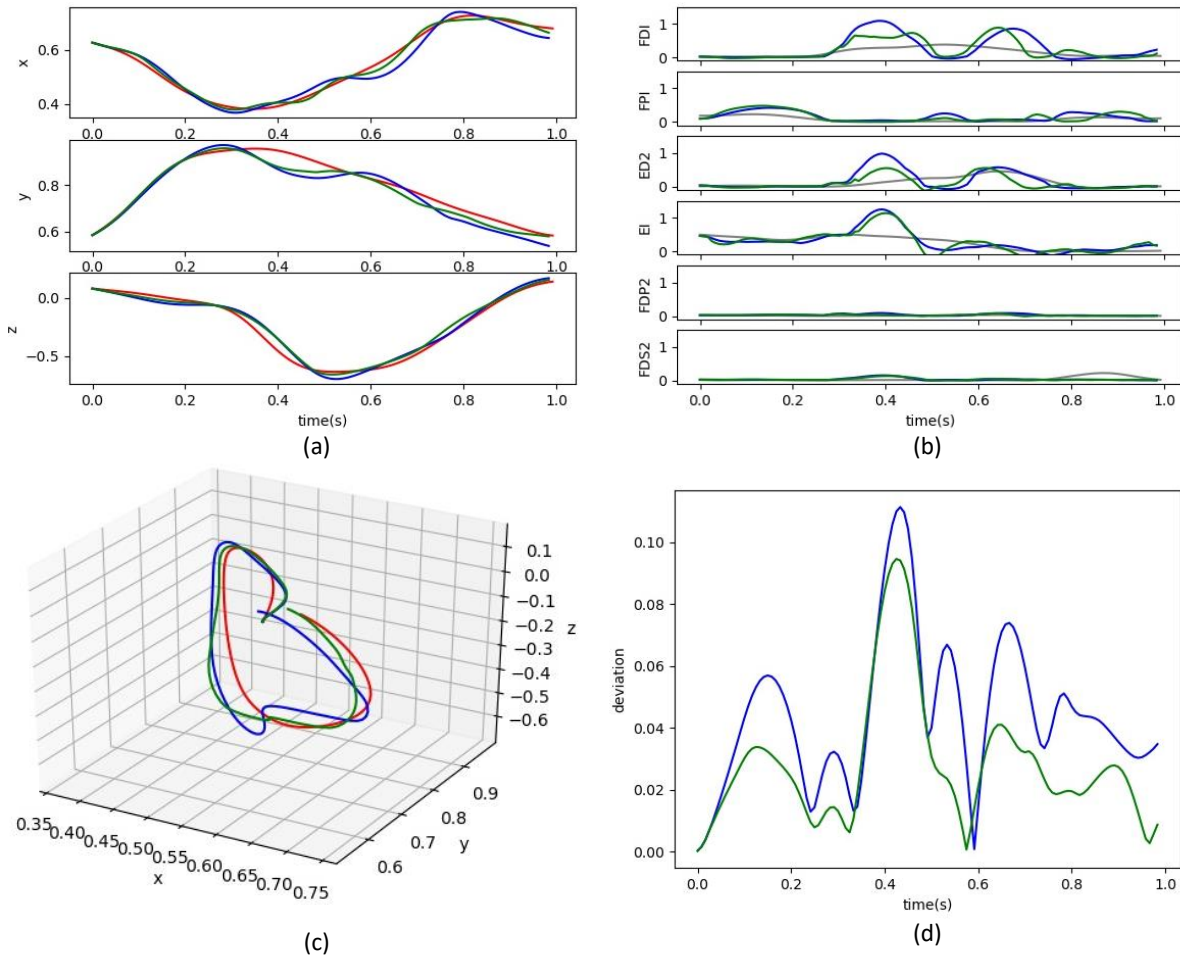


Figure 6. (a) simulated xyz positions given a desired xyz positions, (b) predicted EMG and actual (gray) EMG, (c) the corresponding 3D trajectories, and (d) deviations from the desired trajectory (where blue for simulated outcomes without error compensation, green for simulated outcomes with error compensation, and red for desired in (a)-(d)).

Given the desired path (red), two simulated trajectories (where blue is “without error compensation” and green is “with error compensation”) were presented in Figure 6-(a) and (c). The error compensation allowed us to minimize deviations from the desired path as shown in Figure 6-(d). A simple heuristic was applied to compensate a path following error by adjusting the reference ( $r$ ) whenever  $d \geq \delta$ . The corresponding simulated EMG signals are presented in Figure 6-(b).

Also, we used a longer duration (i.e., 3 seconds) movements as a reference trajectory. While testing, we found several unstable outcomes. Figure 7-(a) shows one example. Due to inaccurate predictions of EMG signals as shown in Figure 7-(b), the system output  $\hat{y}$  diverged. We used normalized EMG signals when the ANN was trained. However, the EMG generator could generate huge values of EMG signals (e.g., FDI > 5). Such errors may have been caused by over-fitting or an inaccurate training data set (see Fig.5). When we add a limiter to the EMG generator (i.e.,  $EMG \leq 1$ ) we could prevent this divergent behavior as shown in Figure 7-(c) and (d).

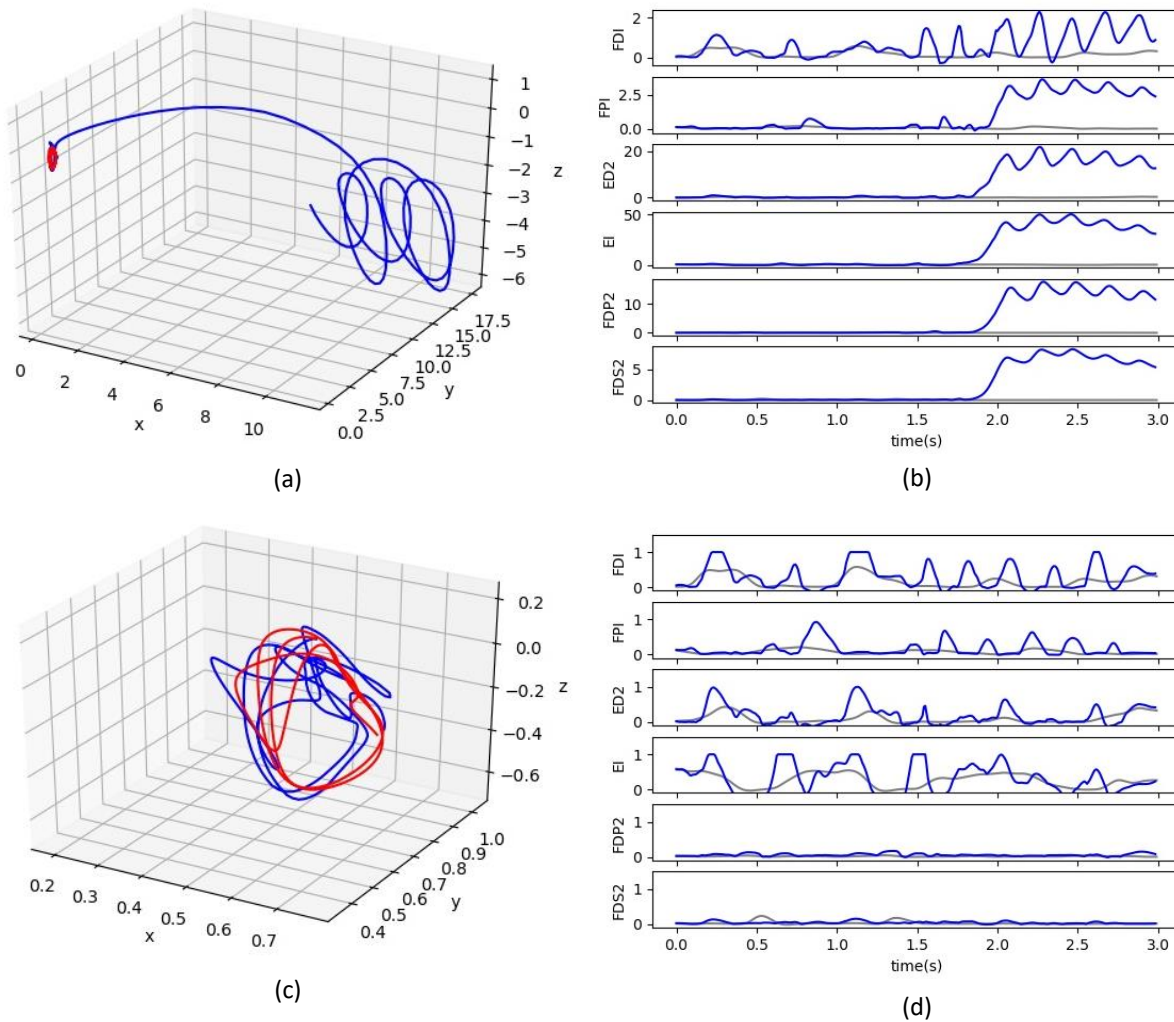


Figure 7. Top two plots show an example of an unstable scenario where (a) trajectories (red for desired and blue for simulated without error compensation) and (b) the predicted EMG (blue) and actual EMG (gray). Bottom two plots show an example of stable scenario after limiting maximum values of EMG where (c) trajectories (red for desired and blue for simulated without error compensation) and (d) the corresponding predicted EMG.

## 5 DISCUSSION

We have shown that the proposed design framework can be used to develop a stable control system associated with prediction of EMG signals given a desired trajectory. The simulation study shows the effectiveness of the proposed approach in terms of system validation. Also, using a simulated system allows us to minimize the likelihood of imposing unphysiological and potentially dangerous levels of activation to a human or animal subject. It may be challenging to demonstrate the stability of a designed controller using conventional stability analysis techniques due to the high complexity of this system. By introducing a simulation-based validation process, we could safely investigate potential risks and erratic behaviors to facilitate design of a stable control system for actual human use.

The proposed framework highly relies on models (i.e., nonlinear system identification and EMG prediction). Therefore, the robustness of the models is important. In our simulation study, we found several limitations of our models such as inaccurate EMG predictions. Due to this, our simple control system was unstable under certain conditions. These poor predictions were likely due to errors in EMG data collection for two of the muscles. Due to data quality, the nonlinear model might also return incorrect estimated positions.

Nevertheless, the initial results show the feasibility of the proposed design framework. However, we need to improve our models for robust simulation. For the improvements, we need to collect more (and valid) data from multiple healthy human subjects because we used data collected from a single subject for this simulation study. We will then extract key muscle activities for a specific movement. Finally, we will redesign our ANNs as needed. For instance, we will investigate introducing an autoencoder architecture for the EMG generator (Li and Li 2021).

Given enhanced and robust models, we will investigate a feedback control strategy (that produces EMG signals as templates for muscle stimulation) to minimize path following errors. The feedback system may be an adaptive controller to make the system more robust. Moreover, we will investigate how to model muscle fatigue, unaccounted position changes, and others to support more complex motions with a large number of muscle activations. Ultimately, we will extend our simulated framework to involve FES converters applied to real limbs.

## ACKNOWLEDGMENTS

Supported by NIH grant R01 NS102259 (to AJF).

## REFERENCES

- Blana, D., R. F. Kirsch, and E. K. Chadwick. 2009. "Combined Feedforward and Feedback Control of a Redundant, Nonlinear, Dynamic Musculoskeletal System." *Medical and Biological Engineering and Computing* vol. 47 (5), pp 533–42. doi:10.1007/s11517-009-0479-3.
- Chen, S., S. A. Billings, and P. M. Grant. 1990. "Non-Linear System Identification Using Neural Networks." *International Journal of Control* vol 51 (6), pp 1191–1214. doi:10.1080/00207179008934126.
- Crago, P. E., R. J. Nakai, and H. J. Chizeck. 1991. "Feedback Regulation of Hand Grasp Opening and Contact Force during Stimulation of Paralyzed Muscle." *IEEE Transactions on Biomedical Engineering* vol 38 (1), pp 17–28.
- Hasse, B., D. Sheets, N. Holly, K. Gothard, and A.J. Fuglevand. 2022. "Restoration of Complex Movement in the Paralyzed Upper Limb." *Journal of Neural Engineering* doi: 10.1088/1741-2552/ac7ad7
- Kilgore, K. L., H. A. Hoyen, A.M. Bryden, R. L. Hart, M. W. Keith, and P. H. Peckham. 2008. "An Implanted Upper-Extremity Neuroprosthesis Using Myoelectric Control." *Journal of Hand Surgery* vol. 33 (4), pp 539–50. doi:10.1016/j.jhsa.2008.01.007.

- Kingma, D. P., and J. Lei Ba. 2014. "Adam: A Method for Stochastic Optimization." In *ArXiv Preprint ArXiv:1412.6980*.
- Li, Z., and S. Li. 2021. "Neural Network Model-Based Control for Manipulator: An Autoencoder Perspective." *IEEE Transactions on Neural Networks and Learning Systems*. doi:10.1109/TNNLS.2021.3109953.
- Lynch, C L, and M R Popovic. 2008. "Functional Electrical Stimulation." *IEEE Control Systems Magazine* vol. 28 (2), pp 40–50.
- Memberg, W. D., K. H. Polasek, R. L. Hart, A. M. Bryden, K. L. Kilgore, G. A. Nemunaitis, H. A. Hoyen, M. W. Keith, and R. F. Kirsch. 2014. "Implanted Neuroprosthesis for Restoring Arm and Hand Function in People with High Level Tetraplegia." *Archives of Physical Medicine and Rehabilitation* 95 (6). Elsevier Ltd: 1201-1211.e1. doi:10.1016/j.apmr.2014.01.028.
- Paszke, A., S. Gross, J. Bradbury, Z. Lin, Z. Devito, F. Massa, B. Steiner, T. Killeen, and E. Yang. 2019. "PyTorch : An Imperative Style , High-Performance Deep Learning Library." In *Proceedings of the 33rd International Conference on Neural Information Processing Systems*, Vancouver, Canada.
- Peckham, P. H., and J. S. Knutson. 2005. "Functional Electrical Stimulation for Neuromuscular Applications." *Annual Review of Biomedical Engineering* vol. 7, pp 327–60. doi:10.1146/annurev.bioeng.6.040803.140103.
- Wenger, N., E. Martin Moraud, Stanisa Raspopovic, Marco Bonizzato, Jack DiGiovanna, Pavel Musienko, Manfred Morari, Silvestro Micera, and Grégoire Courtine. 2014. "Closed-Loop Neuromodulation of Spinal Sensorimotor Circuits Controls Refined Locomotion after Complete Spinal Cord Injury." *Science Translational Medicine* 6 (255): 255ra133-255ra133. doi:10.1126/scitranslmed.3008325.

## AUTHOR BIOGRAPHIES

**MINSIK HONG** is a Research Assistant Professor at the University of Arizona. He holds a Ph.D. in Electrical and Computer Engineering from the University of Arizona. His research interests are robotics, control system, fuzzy theory, and modeling and simulation for medical devices. His email address is [mshong@email.arizona.edu](mailto:mshong@email.arizona.edu).

**BRADY A. HASSE** is a Ph.D. candidate in the Neuroscience Graduate Interdisciplinary Program, working in the Fuglevand lab at the University of Arizona. His research interests are functional electrical stimulation, brain machine interfaces, neural prosthetics, and motor control. His email address is [hasse2ba@email.arizona.edu](mailto:hasse2ba@email.arizona.edu).

**ANDREW J. FUGLEVAND** is professor of Physiology and Neuroscience in the College of Medicine at the University of Arizona. He uses experimental and modeling approaches to understand how the mammalian nervous system controls skeletal muscles to produce coordinated movements. He was the recipient of the Delsys Prize for innovation in electromyography. He has served as a permanent member of the Musculoskeletal and Rehabilitation Sciences NIH study section and associate editor of the Journal of Neurophysiology and Neuroscience Letters. His email address is [fuglevan@email.arizona.edu](mailto:fuglevan@email.arizona.edu).

**JERZY W. ROZNEBLIT** is University Distinguished Professor, Raymond J. Oglethorpe Endowed Chair in the Electrical and Computer Engineering (ECE) Department, with a joint appointment as Professor of Surgery in the College of Medicine at the University of Arizona. During his tenure at the University of Arizona, he established the Model-Based Design Laboratory with major projects in design and analysis of complex, computer-based systems, hardware/software codesign, and simulation modeling. He presently serves as Director of the Life-Critical Computing Systems Initiative, a research enterprise intended to improve the reliability and safety of technology in healthcare and life-critical applications. His email address is [jr@ece.arizona.edu](mailto:jr@ece.arizona.edu).